

RESEARCH ARTICLE

The effects of entombment on water chemistry and bacterial assemblages in closed cryoconite holes on Antarctic glaciers

Jenny G. Webster-Brown^{1,*}, Ian Hawes², Anne D. Jungblut³,
Susanna A. Wood^{4,5} and Hannah K. Christenson^{1,2}

¹Waterways Centre for Freshwater Management, University of Canterbury, Christchurch 8140, New Zealand,

²Gateway Antarctica, University of Canterbury, Christchurch 8140, New Zealand, ³Department of Life Sciences, Natural History Museum, London SW7 5BD, UK, ⁴Cawthron Institute, Nelson 7010, New Zealand and

⁵Environmental Research Institute, University of Waikato, Hamilton 3240, New Zealand

*Corresponding author: Waterways Centre for Freshwater Management, University of Canterbury, Private Bag 4800, Christchurch, New Zealand.

Tel: +64-3-364-2330; Fax: +64-3-364-2365; E-mail: jenny.webster-brown@canterbury.ac.nz

One sentence summary: Glacial closed cryoconite holes contain microbial communities are influenced by both founder populations and water chemistry during the evolution of these unique Antarctic inland aquatic habitats.

Editor: Max Häggblom

ABSTRACT

Closed cryoconite holes (CCHs) are small aquatic ecosystems enclosed in glacier surface ice, and they collectively contribute substantial aquatic habitat to inland Antarctica. We examined the morphology, geochemistry and bacterial diversity of 57 CCHs, spread over seven sites, located on five glaciers, covering a range of latitudes, elevations and distance from open seawater. Isotopes confirmed glacial ice as the initial water source, with water chemistry evolving through freeze concentration and photosynthetic processes to have conductivities ranging from <0.005 to >4 mS cm⁻¹ and pH from <5 to >11 . Nitrate concentrations were more elevated in inland, higher altitude sites. Bacterial communities were characterized by Automated Ribosomal Intergenic Spacer Analysis and high-throughput sequencing. The dominant phyla were Cyanobacteria, Bacteroides, Proteobacteria and Actinobacteria. CCH bacterial communities predominantly grouped by geographic location, suggesting initial wind-borne inocula from local and regional sources play a role in structuring assemblages. However, multivariate multiple regression analysis indicated that internal CCH conditions also influenced community structure, particularly the ion content and pH of the liquid water. This highlights the importance of founder bacterial populations, isolation and water chemistry in the evolution of CCH bacterial communities.

Keywords: Antarctica; bacteria; cryoconite; cyanobacteria; geochemistry; isotopes

INTRODUCTION

Ice is an overwhelming component of continental Antarctic landscapes, but is not lifeless. The falling snow from which it forms contains many previously airborne biological propagules, including Archaea, bacteria, fungi, algae and protozoa,

which can remain viable for long periods of time (Abyzov 1993; Castello and Rogers 2005; Christner *et al.* 2005; Cameron, Hodson and Osborn 2012). Wind also carries dust particles and associated organisms from local ice-free areas and deposits them directly onto snow and ice surfaces (Nkem *et al.* 2006). Glacier ice

surfaces are therefore reservoirs of potentially viable propagules that can become active when they encounter sufficient liquid water of appropriate chemistry.

One of the locations where melted glacier ice and wind-blown particles accumulate is in cryoconite holes. Cryoconites are cylindrical holes in the surface of permanent ice features that are filled with water and have a thin layer of sediment at the bottom. They have been found in the ablation zones of many continental Antarctic glaciers (Hawes, Howard-Williams and Fountain 2008). In these locations, they are a widespread and common aquatic habitat, though as yet largely unquantified in terms of contribution to the polar hydrosphere. Their mechanism of formation and maintenance is well understood. They are initiated when a pocket of sediment accumulates in a small depression on the ice surface, which absorbs solar radiation and melts down into the ice (Wharton et al. 1985; Fountain et al. 2004; 2008). The rate at which this down-melting occurs, and the depth achieved, is largely determined by the distance into the ice to which sufficient solar energy penetrates to sustain basal melting. Year-on-year persistence relies on the sediment pocket melting down in each summer faster than the surface of the ice ablates, and an equilibrium depth of 30–50 cm typically emerges (Gribbon 1979).

Two classes of cryoconite holes are recognized depending on their summer condition; those that open to the air annually, and those that remain closed by a perennial ice lid. In Antarctica, open cryoconite holes occur in ablation zones where glacier surface energy balance is such that the ice is close to melting, and are ubiquitous in warmer regions, such as temperate and arctic glaciers. When the ice lid melts, it allows the liquid phase to equilibrate with the atmosphere and to receive direct deposition of wind- and water-borne material (Mueller et al. 2001). Closed cryoconite holes (CCHs) have only been reported from Antarctica (e.g. Bagshaw et al. 2007; Hawes, Howard-Williams and Fountain 2008; Webster-Brown et al. 2010; Hodson et al. 2013). They form where ablation zones coincide with a surface energy balance such that the ice temperature remains below freezing and the ice lid does not melt. Most information on such holes comes from observations in the Taylor Valley (e.g. Mueller et al. 2001; Tranter et al. 2004; Bagshaw et al. 2007). Gas exchange with the atmosphere is restricted by the persistent ice cap, which can result in unusual carbonate chemistry and extreme pH conditions (Tranter et al. 2004). Because less surface meltwater and windblown particles can enter CCH, dissolved major ions and nutrients dynamics are more dependent on in-hole glacial melt and freeze concentration, weathering of sediment trapped in the hole, and biological activity.

Microbial colonization of cryoconite holes can occur via airborne biological particles, melting glacier ice and, if open periodically, wind and water delivery. Trophic webs tend to be simple, with algae and cyanobacteria the primary producers and

heterotrophic bacteria and fungi thought to act as recyclers (Porazinska et al. 2004; Foreman et al. 2007). Despite their simplicity, they can contribute considerable biological productivity to the otherwise life-poor cryosphere (Hodson et al. 2008; Anesio et al. 2009).

CCHs thus represent unusual environments, entombed in ice and largely isolated from the outside world. They are the cryospheric equivalents of island ecosystems, and the chemistry and, depending on their degree of connectivity, the community composition that evolves in these isolated habitats is likely to be influenced by stochastic colonization events (i.e. founder effects—Waters, Fraser and Hewitt 2013) in their early development. They offer a unique opportunity to test questions regarding factors controlling the composition of microbial communities in Antarctica, particularly the relative importance of selection by growth environment versus stochastic effects on the colonizing populations.

In this study, we surveyed CCHs at six sites on four glaciers of different latitude, altitude and distance from the sea in Southern Victoria Land, Antarctica (Table 1, Fig. 1). Two sites were sampled on the Lower Koettlitz. The sites were selected to incorporate a range of different physical, biological and chemical CCH habitats. We also included data from a previous study on CCH at the Lower Darwin Glacier (Webster-Brown et al. 2010) to enhance coverage. We aimed to test three hypotheses;

- (i) There is greater variability in CCHs physical environments between glacier sites and latitudes, than within a site, due to local differences in external environmental conditions.
- (ii) There is greater variability in CCHs chemical characteristics within the different glacier sites, than between sites, due to factors linked to individual CCH genesis and evolution.
- (iii) Bacterial assemblages within CCHs are primarily derived from a common airborne pool of propagules in the Southern Victoria Land region, rather than from local sources, so that bacterial assemblages are similar for glaciers where similar growth conditions occur.

METHODS

Study area

CCHs were sampled on gently sloping ablation zones on the Upper and Lower Wright Glaciers, the upper and lower parts of the Koettlitz Glacier and the Diamond Glacier (Fig. 1, Table 1). Additionally, data from Webster-Brown et al. (2010) for CCH on the Lower Darwin Glacier were included in our analysis (Fig. 1, Table 1). The Upper Wright Glacier drains the polar ice cap, entering the Wright Valley via an ice fall. The Lower Wright Glacier is at the opposite (eastern) end of the Wright Valley, and is derived from the Wilson coastal piedmont system. The Koettlitz Glacier drains a catchment separate from the main ice cap. The Upper

Table 1. Attributes of the seven glacier collection sites, and sampling period in Southern Victoria Land.

Location	Latitude/longitude	Distance to sea (km)	Altitude (m)	Sampling season
Diamond	79° 50'S, 159° 00'E	260	600	December 2010
Lower Darwin ^a	79° 49'S, 159° 40'E	240	100	January 2007
Upper Koettlitz	78° 18'S, 163° 38'E	80	800	January 2010
Lower Koettlitz (edge)	78° 10'S, 165° 03'E	40	30	January 2010
Lower Koettlitz (centre)	78° 08'S, 164° 14'E	35	30	January 2013
Upper Wright	77° 27'S, 162° 52'E	75	950	January 2012
Lower Wright	77° 32'S, 160° 43'E	20	450	January 2012

^aSampled and some results reported by Webster-Brown et al. (2010).

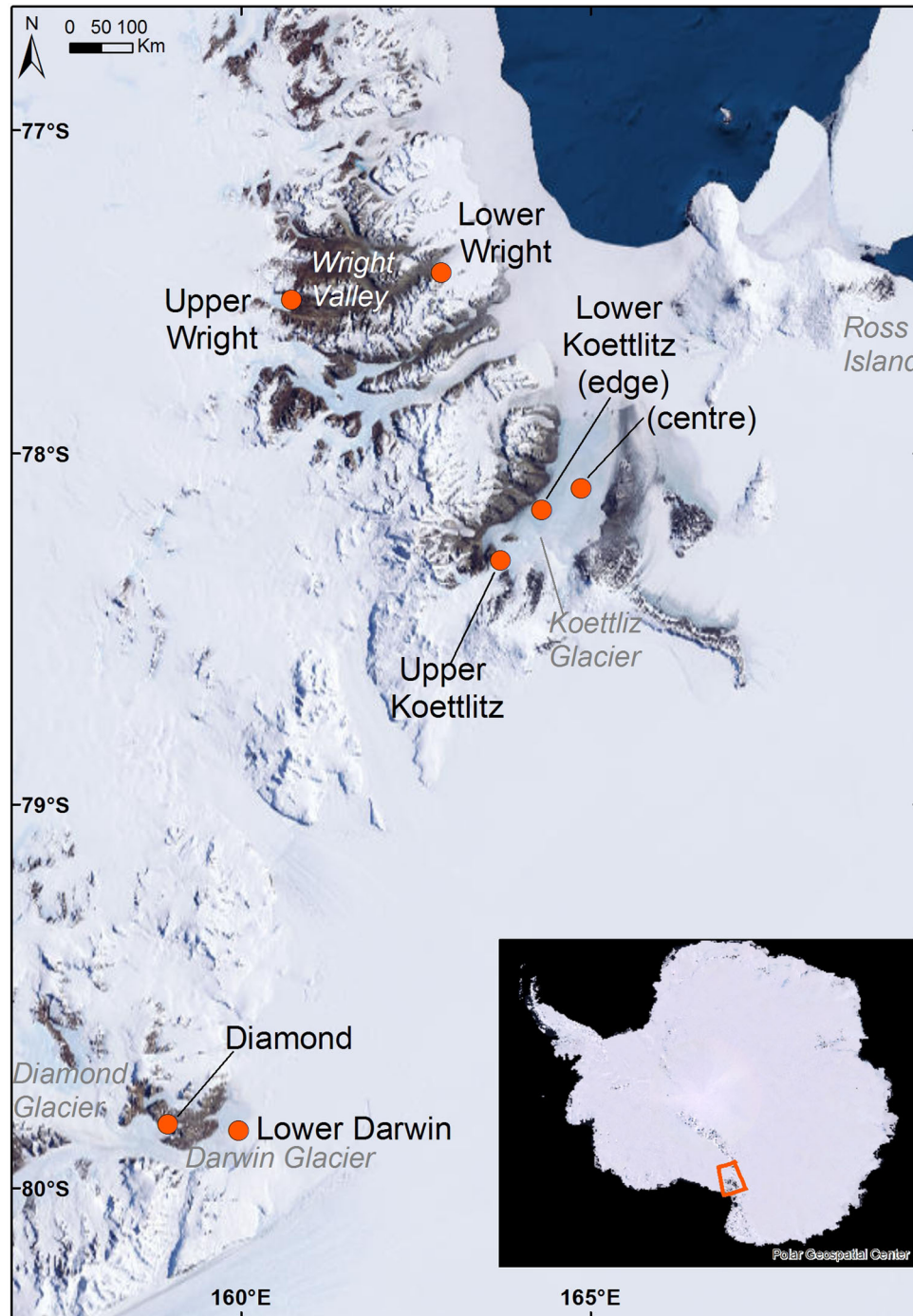


Figure 1. Location of seven study areas in Southern Victoria Land, Antarctica.

Koettlitz Glacier site was located towards the top of the ablation zone, and Lower Koettlitz Glacier site was relatively close to the open sea, and only slightly above sea level, where the glacier may be floating on the seawater in the McMurdo Sound. At the latter site, two locations were sampled; one close to the northern edge, accessible by foot, and one in the centre of the glacier, accessible only by helicopter (Fig. 1). The Darwin Glacier drains the inland ice cap, but the Lower Darwin Glacier is close to sea level despite being over 200 km inland from where the glacier merges with the Ross Ice Shelf (Table 1). The Diamond Glacier is a terminal branch of the Upper Darwin Glacier. At the Lower Darwin

Glacier site, large pools and streams of meltwater were observed in the cryoconite field at the time of sampling. These pools engulfed some cryoconite holes, and while those chosen were isolated and closed at the time of sampling, we cannot be sure that this was the case in previous summer seasons (Webster-Brown et al. 2010).

Sampling

Cryoconite holes were sampled in the austral summer (December–January), during Antarctic field seasons between

2010 and 2013 (Table 1). An initial survey of 39 cryoconites at the Upper Koettlitz Glacier site, over a wide range of diameter (5–80 cm), revealed that only those with a diameter of greater than 30 cm (which were typically also greater than 35 cm deep) routinely contained liquid water. These became the ‘target size’ CCHs to be sampled. Each sampling targeted at least five CCHs per site with a diameter of 30–100 cm (actual number 5–12, see results tables). Selection was based on replicate N+1 being the next encountered appropriately sized CCH encountered in a random direction from replicate N. Access through the ice lid was accomplished using a 50-mm diameter Kovacs ice drill, which was cleaned between each hole with antibacterial wipes. On penetrating the ice cover, characteristics of the CCH were recorded (diameter, depth, ice thickness, presence/absence of water and depth of air gap between ice and water). The temperature, pH, dissolved oxygen (DO) and conductivity were measured *in situ* using a calibrated HACH 40D multimeter. Water samples were collected directly into three 60-mL centrifuge tubes for determination of major ions and isotopes, using a manual vacuum apparatus. A sample (1 L) was collected by vacuum into an acid-washed PVC bottle. Three sub-samples (2 mL each) were taken immediately and injected through rubber septa into 12-mL gas-tight tubes pre-loaded with concentrated phosphoric acid (0.2 mL) for later determination of dissolved inorganic carbon (DIC) as carbon dioxide (CO₂). The volume of water remaining in the CCH was determined using a measuring cylinder, and a subsample (100 mL) filtered (Whatman GF/F) into an acid-washed polyethylene bottle and frozen for later nutrient analysis.

Sediment samples for molecular analysis were collected into 60-mL centrifuge tubes using a sterile spatula, and frozen. In addition, the total amount of sediment of three further CCHs of 40–50 cm diameter, which had not previously been sampled, was determined for the Upper Koettlitz site. The ice lid was removed, allowing the total volume of liquid water to be determined and sediment to be excavated for later drying and weighing.

Chemical analysis

Water samples were analysed for sodium (Na), potassium (K), calcium (Ca) and magnesium (Mg) by Inductively Coupled Plasma-Mass Spectrometry (ICP-MS) for which detection limits were 0.02 mg L⁻¹ for Na and Mg, and 0.05 mg L⁻¹ for Ca and K. Samples for chloride (Cl) and sulphate (SO₄), were analysed by high-performance ion chromatography (HPIC), with detection limits of 0.1 and 0.05 mg L⁻¹, respectively. DIC was measured by injecting a subsample of the acidified headspace, from the gas-tight sample tubes, directly into a stream of nitrogen gas, which then passed through the measuring channel of a Li-Cor Li-720 infra-red gas analyser, with a detection limit of 0.1 mg L⁻¹. These data were converted to bicarbonate ions for reporting purposes, and to calculate ion balances which were mainly less than 5%, and always less than 10%.

For nutrient analyses, nitrate nitrogen (NO₃-N), ammoniacal nitrogen (NH₄-N) and dissolved reactive phosphorous (DRP) were measured using an Astoria autoanalyser. With this technique, the NO₃-N analysis includes any nitrite (NO₂-N) present. The latter was not determined separately as previous studies showed this to be a small proportion to the total nitrogen budget in similar waters (Vincent and Howard-Williams 1994). Total dissolved N (TDN) and P (TDP) were determined after digestion as NH₄-N and DRP respectively using a Lachat flow injection analyser. Dissolved organic N (DON) and P (DOP) were determined from TDN and TDP by subtraction of inorganic forms. The de-

tection limit for TON and TOP was 1 µg L⁻¹; DRP and DOP concentrations were commonly at or below this limit.

Stable isotopes were determined using mass spectrometry (by GNS, Wellington, New Zealand) on unfiltered water samples; 50 mL for ¹⁸O and ²H (deuterium, D), and 1 L for ³H (tritium).

DNA extractions and molecular analysis

We used a three-tiered approach. Bacterial- and cyanobacterial-specific Automated Ribosomal Intergenic Spacer Analysis (ARISA) was used to investigate community structure at all sites. A subset of these were selected for in-depth taxonomic assessment using high-throughput sequencing (HTS). Difficulties with insufficient DNA or amplification of DNA prevented the analysis of the full sample set using this technique. Finally, a subset of samples were also analysed using a cyanobacterial specific 16S rRNA clone-library approach to specifically investigate phylogenetic relationships with other taxa previously characterized from Antarctica.

DNA was extracted from sediment using the MoBio Power Soil kit (USA). ARISA PCR reactions using cyanobacterial-specific primers CY-ARISA-F and 23S30R (Wood *et al.* 2008) and bacterial primers ITSF and ITSReub (Cardinale *et al.* 2004), followed the protocols described in Wood *et al.* (2012a,b). Amplicon lengths were resolved on an ABI 3130xL Genetic Analyzer (PE Applied Biosystems, USA) run under GeneScan mode at 15 kV for 45 min according to the manufacturer's instructions. Each sample contained 0.25 µL of internal GS1200LIZ ZyStandard (PE Applied Biosystems, USA). The resulting electropherograms were processed using the PeakScanner software v1.0 (Applied Biosystems, USA) and an in-house pipeline modified from Abdo *et al.* (2006) written using Python 2.7.1 (Python Software Foundation) and R (<http://www.r-project.org>). Bacterial ARISA data from Webster-Brown *et al.* (2010) from the Lower Darwin Glacier were included.

Based on ARISA data, specific samples from the Diamond Glacier (representing high- and low-pH regimes), the Lower Koettlitz Glacier (edge and centre samples) and the Upper Koettlitz Glacier were chosen for HTS analysis. A region of the 16S rRNA gene covering the V3 and 4 sections was amplified by PCR (iCycler; Biorad) using bacterial-specific primers 515F and 806R (Caporaso *et al.* 2011). PCR reactions were performed in 50 µL volumes with the reaction mixture containing; 45 µL of Platinum® PCR SuperMix High Fidelity (Life Technologies, USA), 10 µM of each primer, and 10–20 ng of template DNA. The reaction mixture was held at 94°C for 2 min followed by 27 cycles of 94°C for 30 s, 54°C for 30 s, 68°C for 45 s, with a final extension step at 68°C for 5 min. PCR products were purified (Agencourt® AMPure® XP Kit; Beckman Coulter, USA), quantified (Qubit® 20 Fluorometer, Life Technologies, USA), diluted to 1 ng µL⁻¹ and submitted to New Zealand Genomics Limited (Auckland, New Zealand) for library preparation. Libraries were sequenced on a MiSeq Illumina platform (2 × 250 reads).

Illumina datasets were demultiplexed using MiSeq Reporter v2.0. All further analysis was performed using MOTHUR (Schloss *et al.* 2009). The sequences corresponding to the forward and reverse primers were trimmed, and merged into single contigs (maximum length of 292 nucleotides). Contigs were aligned to the SILVA bacteria reference alignment (Pruesse *et al.* 2007) and chimera removal performed using the UCHIME algorithm (Edgar *et al.* 2011). Sequences were clustered in operational taxonomic units (OTUs) using 0.02 pairwise sequence distance cut-off values. To account for differential sequencing depth among samples, the number of reads in each sample was rarefied

(randomly down-sampled) to 33 898 reads per sample. OTUs represented by less than 10 reads across all samples were removed. OTUs were then classified to identify taxonomic annotation using the Greengenes taxonomic database (McDonald et al. 2012). Sequences of unknown, archaeal or eukaryotic origin were removed. Raw sequences are available at the National Center for Biotechnology Information Sequence Read Archive under the accession number PRJNA296701.

Nine clone libraries were constructed from selected samples from the Upper Koettlitz, Diamond and Lower Wright Glaciers to cover the range of observed pH conditions. PCR amplification of cyanobacterial 16S rRNA genes was performed using 1 unit Platinum Taq DNA Polymerase High Fidelity (Life Technologies, UK) in a 20 μ L reaction, as described in Jungblut, Lovejoy and Vincent (2010). The cyanobacteria 16S rRNA gene primers were 27F1 (5'-AGAGTTTGATCCTGGCTCAG-3') and 809R (5'-GCTTCGGCACGGTCTCGGTCGATA-3') (Jungblut et al. 2005). PCR products were purified (Qiagen, Germany) and cloned using the Stragene cloning kit (Stratagene, USA) following the manufacturer instructions. Positive clones were transferred to 96-well plates containing Luria Bertani medium with 7% glycerol (Jungblut, Lovejoy and Vincent 2010). The inserted 16S rRNA sequences were amplified using vector-specific primers M13f and sequenced using the vector-specific T7 universal primer at the Natural History Museum sequencing facility using an Applied Biosystems 3730xl DNA analyser (Applied Biosystems, USA).

Sequences were checked for chimeras using Bellerophon (Huber, Faulkner and Hugenholz 2004), and these were excluded from further analysis. Sequences were edited using 4peaks and aligned using Clustalw (Larkin et al. 2007). Manual editing was carried with MacClade 4.08 (Maddison and Maddison 2005). OTUs were defined as groups of sequences that were at 97% similar using MOTHUR (Schloss et al. 2009). For each OTU, a closest cultured and uncultured match based using a BLASTn search (14 May 2014, Altschul et al. 1990) to GenBank was undertaken and these were used in phylogenetic analysis. A phylogenetic tree was constructed using maximum likelihood with RAXML-HPC2 on TG (7.2.8; CIPRES Science Gateway V 3.0, Stamatakis, Hoover and Rougemont 2008 as described in Jungblut, Vincent and Lovejoy 2012). For context, we also searched for 16S rRNA gene sequences from isolates of the identified morphotypes and environmental 16S rRNA gene sequence data from other Arctic and Antarctic sites for inclusion in phylogenetic trees. The 16S rRNA gene sequences are available under GenBank accession numbers KT424925- KT424941.

Statistical analysis

Analysis of variance was used with physical data to determine whether significant differences occurred between study sites. No transformations were necessary to meet normality criteria. Where differences were apparent, *post hoc* testing using a Holm-Sidak pairwise comparison were used to identify where significant differences lay.

ARISA results were transformed to presence/absence data. Differences in bacterial and cyanobacterial community structure (ARISA data) between sites were visualized by principal coordinate (PCO) analyses and tested using permutational multivariate analysis of variance (PERMANOVA; Anderson 2001) using Bray-Curtis similarities, type III sums of squares and permutation of residuals under a reduced model. Differences in multivariate dispersion between sites were tested using PERMDIST and *post hoc* pairwise comparisons were undertaken using a pairwise PERMANOVA *t*-test. All tests used 9999 permutations.

All further analysis was undertaken only on bacterial ARISA as this was the most comprehensive dataset. The relationship between ARISA bacterial community structure and environmental variables was analysed using multivariate multiple regression (McArdle and Anderson 2001), using the DistLM routine in the PRIMER 6 and PERMANOVA (Anderson and Gorley 2007). A marginal test was used where individual variables were fitted separately to test their relationship with the bacterial ARISA data (ignoring other variables), followed by a stepwise selection procedure, conditional on variables already included in the model and using the AICc selection criteria. The conditional test identifies the subset of variables that best predicts the observed pattern in bacterial ARISA community structure. Both the conditional and marginal tests were undertaken with 4999 permutations using Bray-Curtis similarities. Draftsmans plots were used to check multicollinearity and skewness among predictor variables. Several predictor variables were transformed before analyses to meet the assumption of homogeneity of dispersion. Environmental variables used in the analyses were DO, pH, Sqrt(HCO₃), Log(Na+0.1), Log(Ca+0.1), Log(DRP+0.1), Log(NH₄+0.1), Log(NO₃+0.1), Log(DON+0.1), Log(DOP+0.1), distance to sea and altitude. Highly collinear variables ($r^2 > 0.9$) were not considered in the analysis, including Cl, SO₄, K, Mg, TDN and TDP. The resulting model was visualized using distance-based redundancy analysis (Legendre and Anderson 1999), where the ordination axes are linear combinations of the environmental variables that maximally explain biotic variation.

Species richness (R), Shannon-Wiener diversity index (H') and Pielou evenness index (J) were calculated for HTS data using the DIVERSE function in PRIMER 6. The HTS OTU data were fourth root transformed and analysed using non-metric multidimensional scaling (MDS) based on Bray-Curtis similarities with 100 random restarts and results were plotted in two dimensions. Agglomerative, hierarchical clustering of the Bray-Curtis similarities was undertaken using the CLUSTER function of PRIMER 6 and plotted onto the two-dimensional MDS plots. Relative taxa abundance was visualized with heat maps constructed using R (<http://www.r-project.org>).

RESULTS

Cryoconite morphology

The morphology of Upper Koettlitz Glacier CCHs in the target range, averaged over nine such cryoconites, is shown in Fig. 2. This illustrates the key attributes of a water-containing CCH, and acts as a reference for Table 2. Across all of the glacier sites, broad similarities in the depth to the sediment and thickness of the ice lid were observed in CCHs (Table 2). The Lower Wright and Lower Koettlitz Glacier sites had significantly (ANOVA, $P < 0.05$) thinner ice cover than the analogous upper glacier sites, particularly for the Lower Koettlitz (edge) site where some holes had very thin or partial lid ice (Table 2). Lower Wright and Lower Koettlitz Glacier (edge) CCHs also appeared shallower on average than at other sites, but this difference proved not to be statistically significant (ANOVA, $P > 0.05$).

The sediment content of the three CCHs on the Upper Koettlitz Glacier that were completely deconstructed for water and sediment content yielded an average sediment cover of 1.4 g cm⁻². The sediment appeared to be predominantly dolerite and quaternary volcanic (including scoria) lithologies, with particle sizes ranging from 1 mm to 1 cm, with occasional plate-like rock fragments up to 4 cm across. Rock fragments lacked evidence

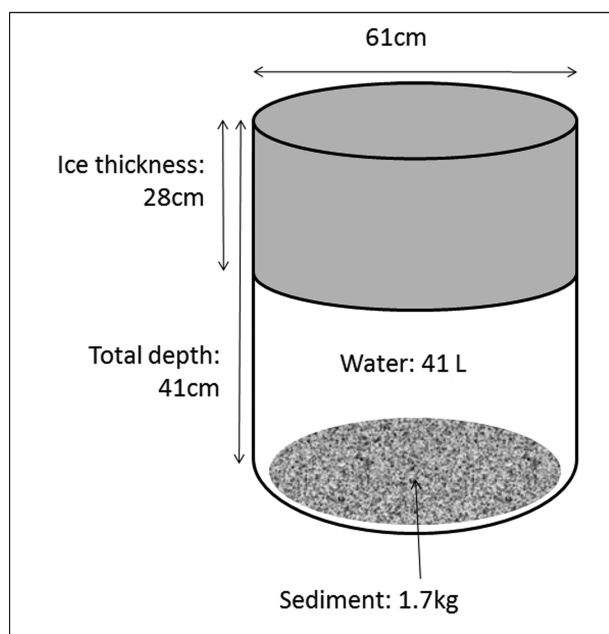


Figure 2. The morphology of an 'average' cryoconite from the Upper Koettlitz Glacier.

Table 2. Depth and ice thickness of sampled cryoconite holes, in the 30–100 cm diameter target range. Data are means \pm one standard deviation.

Location Elevation (masl)	Diameter (cm)	Depth (cm)	Ice thickness (cm)	Number (N)
>500				
Upper Koettlitz	61 \pm 14	41 \pm 3	28 \pm 5 ^{a,b}	9
Diamond	66 \pm 17	43 \pm 7	30 \pm 6 ^a	11
Upper Wright	47 \pm 10	42 \pm 7	36 \pm 6 ^a	7
<500				
Lower Wright	35 \pm 8	33 \pm 4	25 \pm 4 ^b	6
Lower Darwin	59 \pm 29	43 \pm 11	32 \pm 22 ^{a,b}	12
Lower Koettlitz (edge)	37 \pm 15	34 \pm 7	3 \pm 2 ^c	7
Lower Koettlitz (centre)	48 \pm 8	43 \pm 9	21 \pm 14 ^b	5

^{a-c}Values of ice thickness with the same letters are not significantly different by ANOVA. There were no significant differences between sites for depth.

of glacial derivation (e.g. fine particle size or scoured surfaces), and the size distribution was more consistent with a predominantly aeolian origin. Clasts were also predominantly rounded in shape, consistent with aeolian transport, rather than angular as they would have been if carved by glacial erosion.

Meltwater geochemistry

While water chemistry was highly variable, most CCHs had a conductivity of $<200 \mu\text{S cm}^{-1}$ and those on the Lower Darwin Glacier were consistently $<10 \mu\text{S cm}^{-1}$ (Table 3, Fig. 3). The highest conductivities were found in Lower Koettlitz Glacier cryoconites with thin ice cover at the time of sampling, particularly those near the centre of the glacier. Overall pH ranged from 4.80–11.97, with differences of between 0.5 and 6 units observed in the CCHs of each site. There was no consistent relationship between pH and conductivity across all of the sites but (overlapping) pH-conductivity groupings were evident for each site (Fig. 3), with low pH (<6.5), moderate conductivity for the Upper and Lower

Wright Glaciers, moderate pH (7–9) and very low conductivity ($<10 \mu\text{S cm}^{-1}$) for the Lower Darwin Glacier, moderate pH and high conductivity on the Lower Koettlitz and high pH (>9), and moderate conductivity for the Upper Koettlitz Glacier site. On the Diamond Glacier the conductivity was also moderate ($<500 \mu\text{S cm}^{-1}$), but a large range in pH (from 5.5 to 11.8) was evident, with high- and low-pH CCHs occurring within a few meters of each other. Temperatures were uniformly 0°C – 3.1°C in all CCHs.

The chemistry of most CCHs was Na-Cl ion dominated, with Ca and HCO_3^- making a significant contribution to major ion chemistry only at the Upper Koettlitz (where 5 of 9 CCHs were Ca-Na- HCO_3^- dominated) and at the Diamond Glacier (where 3 of 11 were Ca-Na-Cl dominated). Nitrate made a substantial contribution to major ion chemistry ($>20\%$ of anions) in CCHs of the Diamond, Lower Darwin and Upper Wright Glacier sites.

Covariance with conductivity was close to linear for Cl (Fig. 3), and across all sites, strong correlations with Cl ($r^2 > 0.90$) were demonstrated for Na, Mg and K ($r^2 = 0.99$). This indicates elevated concentrations of these ions may be solely due to those processes also affecting the conservative Cl ion, such as freeze concentration, evaporation and/or marine aerosol entrainment. Similarly strong correlations with Cl were also seen for Ca and NO_3^- , at the Upper and Lower Wright Glacier sites, and to a lesser degree ($r^2 = 0.75$ and 0.80 , respectively) at Diamond Glacier site, indicating that Ca and NO_3^- can also be elevated by such processes. However, the Lower Koettlitz Glacier CCHs had consistently lower Ca and NO_3^- concentrations than CCHs of similar conductivity at other sites, while the Upper Koettlitz Glacier site had two distinct groups of CCHs of relatively high or low NO_3^- concentrations (shown on Fig. 3). Bicarbonate showed no correlation with conductivity (data not shown).

Isotope geochemistry

Stable oxygen and hydrogen (^{18}O and D) were measured in CCH water as well as in adjacent glacier ice (Fig. 4). Distribution along the meteoric fraction line shows the glacial ice and CCH water have similar degree of fractionation for each site, and that sites of highest elevation and latitude have the greatest enrichment in lighter isotopes. Those of lower elevation are relatively enriched in the heavier isotopes, particularly those at sea level on the Lower Koettlitz Glacier, where all have an isotopic signature similar to that of standard mean ocean seawater.

Tritium isotopes were also measured in a single CCH at two sites; on the Diamond Glacier where CCH TU = 0.152, and on the Upper Koettlitz Glacier where CCH TU = 0.036. A similarly low tritium concentration was measured in a sample of Diamond Glacier ice; TU = 0.216.

Meltwater nutrients

Detectable amounts of fixed N were present at all sites and, as noted above, particularly high concentrations of NO_3^- were observed in the Upper Wright and Diamond Glacier sites, while NO_3^- formed a high proportion of total ions on the Lower Darwin (Table 3, Fig. 3). Ammonium was always less abundant than NO_3^- -N, and DON was detectable in most samples and particularly high in some of the Diamond Glacier CCHs. Dissolved reactive phosphorus and DOP were generally present at concentrations close to detection limits, except for a few cryoconites on the Diamond and Upper Koettlitz Glaciers, with DRP above 270 and $360 \mu\text{g L}^{-1}$, respectively (Table 3).

Table 3. The range of chemical characteristics measured in cryoconite holes containing liquid water, at each of the glacier sites. Units for conductivity are $\mu\text{S cm}^{-1}$, major ions mg L^{-1} and forms of nitrogen and phosphorus $\mu\text{g L}^{-1}$. The number of cryoconite holes sampled at each site is shown in parenthesis. U = Upper, L = Lower.

Location	Conductivity	Dissolved Oxygen	pH	Na	K
Diamond (11)	5.6–500	15.8–>20	5.68–11.58	1.65–47	0.65–5.4
L. Darwin (10)	2.7–6.6	15.6–20	7.44–9.21	0.08–0.36	<0.05–0.14
U. Koettlitz (9)	16–112	13.8–16.2	9.07–11.97	0.75–4.3	0.23–1.2
L. Koettlitz (edge:6)	88–482	9.2–12.8	8.07–10.01	19–85	0.93–3.4
L. Koettlitz (centre:5)	648–4230	11.3–14.2	9.19–9.72	100–770	3.8–22
U. Wright (7)	26–197	14.5–>20	5.47–8.25	2.9–19	0.17–0.61
L. Wright (6)	12–175	13.9–18.9	4.80–5.80	2.4–12	0.40–1.5
	Ca	Mg	Cl	SO₄	HCO₃
Diamond (11)	1.3–48	0.06–15	2.2–87	4.4–142	0.59–17
L. Darwin (10)	0.06–0.22	0.02–0.07	0.13–3.3	0.52–1.13	4.3–8.1
U. Koettlitz (9)	1.3–10.7	0.19–0.51	1.1–6.8	2.8–12.7	1.8–13
L. Koettlitz (edge:6)	0.78–3.3	1.6–6.7	33–149	4.9–50	2.1–5.6
L. Koettlitz (centre:5)	3.9–27	8.9–76	163–1100	37–350	9.7–14
U. Wright (7)	1.9–11.1	1.1–7.2	2.0–17	4.8–33	0.58–5.2
L. Wright (6)	0.62–6.7	0.38–4.1	3.5–20	1.9–18	<0.1–2.8
	NO₃-N	NH₄-N	DON	DRP	DOP
Diamond (9)	324–5810	4–31	<1–2040	<1–276	1–19
L. Darwin (10)	12–92	1–7	48–560	<1–6	<1
U. Koettlitz (9)	4–88	2–15	43–229	5–367	4–44
L. Koettlitz (edge:6)	<1–10	7–47	67–130	5–22	<1–11
L. Koettlitz (centre:5)	<1 (all)	3–6	84–226	11–22	6.1–11
U. Wright (4)	676–1790	6–23	<1–41	<1–2	1–2
L. Wright (6)	19–567	14–33	17–412	<1–5	1–3

Bacterial and cyanobacterial community structure by ARISA

Analysis of ARISA data for all samples identified a total of 603 distinct bacterial and 55 distinct cyanobacterial ARISA fragment lengths (AFLs; i.e. peaks). Samples from the Lower Koettlitz Glacier (centre) contained the highest average number of AFL (Table S1, Supporting Information). Ordination of the ARISA data for both bacterial and cyanobacterial assemblages showed that in general bacterial assemblages clustered according to their geographic location, with the two different sites on the Lower Koettlitz Glacier clustering together (Fig. 5). The only exceptions were the Upper Diamond and Upper Koettlitz Glacier sites, which clustered together in both the bacterial and cyanobacterial PCOs (Fig. 5). Additionally, three samples from Upper Diamond Glacier analysed with the bacterial ARISA, formed a tight cluster quite separate from all other samples (Fig. 5a).

Bacterial and cyanobacterial community structure differed significantly among sites (PERMANOVA, $F = 6.96$, $P = 0.0001$ and $F = 10.42$, $P = 0.001$). Pairwise test showed bacterial community structure differed between all sites (pairwise PERMANOVA, $P < 0.01$ for all) except Upper and Lower Wright, and Lower Koettlitz (edge and centre) and Upper Wright (Table S2, Supporting Information). Fewer differences were observed among sites for the cyanobacterial community structure data (Table S2, Supporting Information).

The multivariate regression analysis showed that all environment variables individually had a significant relationship with bacterial community structure, except DON (Table 4). The greatest amount of variation was explained by Na (11.7%) and pH (11.2%), which tended to create two dominant ordination axes (Fig. 6). The sequential model showed that the six variables together explained 46.7% of the total variation of bacterial com-

munity structure (Table 4). Although Na explained the largest proportion of variability, similar results are expected with conductivity, Cl, K and Mg which were highly correlated with Na and so were removed from the analysis (see methods). Redundancy analysis ordination plots indicate that the bacterial communities across sites were correlated with differing environmental variables. For example, the bacterial communities in Darwin CCH were strongly related to DO (Fig. 6). In contrast, assemblages in CCH from the Lower and Upper Wright and three Diamond CCH corresponded strongly with increased altitude and low pH (Fig. 6). The Lower Koettlitz communities both correlated with increased Na and to a lesser extent DOP (Fig. 6).

HTS analysis of sediments in cryoconite holes

HTS was applied to cryoconite sediments from Upper (three CCHs) and Lower Koettlitz edge (six CCHs) and centre (four CCH) and Diamond Glaciers (six CCHs). Due to the clear differences seen in ARISA analyses, Diamond Glacier CCHs were divided into those above and below pH 6 for comparison. Bioinformatics analysis resulted in the clustering of sequences into 1949 OTUs. Samples from the Lower Koettlitz Glacier (edge) contained the most OTUs and highest species richness, Shannon–Wiener Index and Pielou Index (Table 5). In general, ordination of these data showed similar trends as the ARISA with clustering of samples based strongly on their geographic location (Fig. S1, Supporting Information), with the Upper Diamond site samples still showing variability both in bacterial and cyanobacterial composition with pH.

Cyanobacteria were the dominant phylum in samples from the Diamond (pH > 6, 39%), Lower Koettlitz edge (35%) and Upper Koettlitz (29%), whereas Bacteroidetes were most abundant in Lower Koettlitz centre (42%; Fig. 7). In contrast, the Diamond

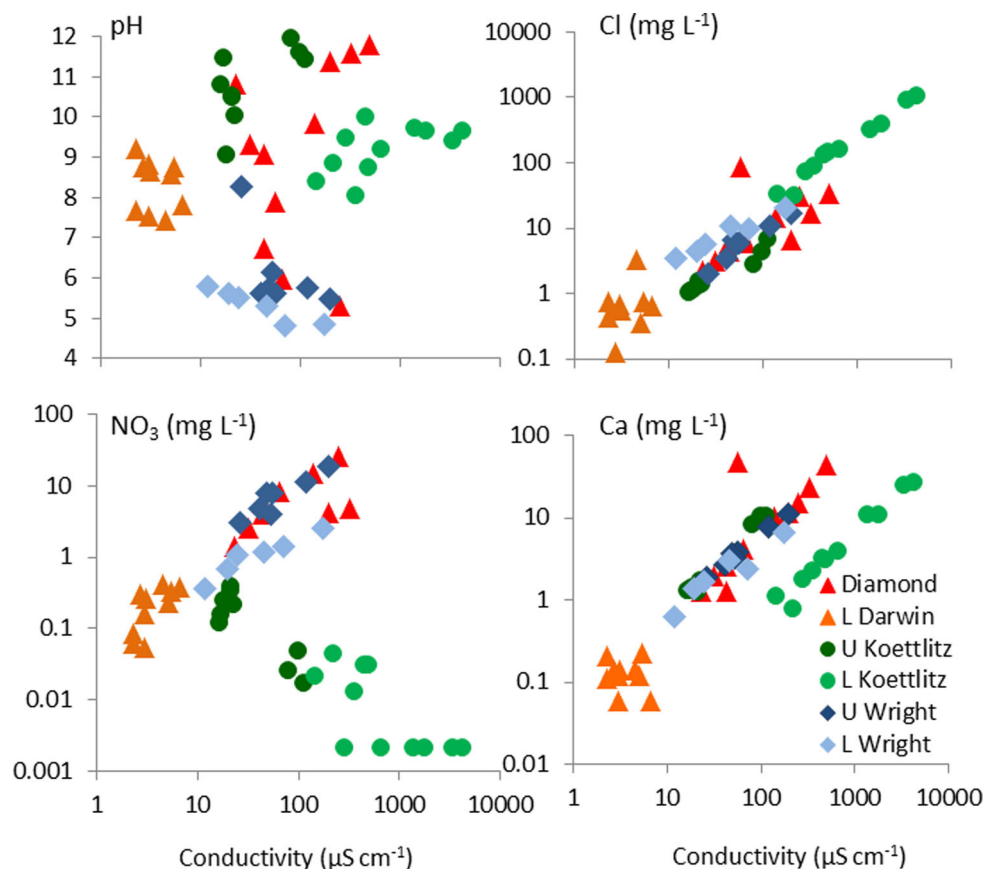


Figure 3. Selected chemical characteristics as a function of conductivity, for cryoconite holes at each of the study areas. Nitrates on lower right of plot are below detection limits. Cl = chloride, NO₃ = nitrate, Ca = calcium, U = Upper, L = Lower.

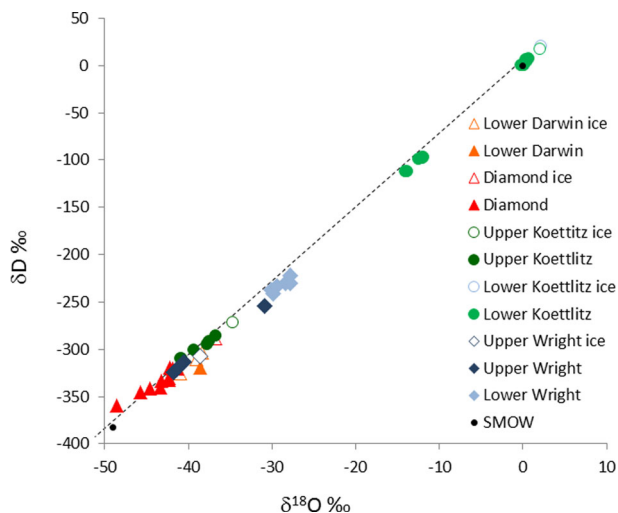


Figure 4. Stable isotopes in CCH water from each of the study sites. The fractionation line for standard mean ocean seawater (SMOW), along which water undergoing fractionation due to evaporation and meteoric precipitation can be expected to plot, is shown as the dashed line between two black points.

Glacier CCH with pH < 6, were dominated by Proteobacteria (50%), followed by Actinobacteria (17%; Fig. 7) and contained relatively few cyanobacteria (Fig. 7). Among Bacteroidetes, Cytophagales were dominant at all sites except Upper Koettlitz where Saprospira was the most abundant order (Fig. S2, Sup-

porting Information). The most dominant Proteobacteria were Burkholderiales at Diamond Glacier (pH > 6), Lower Koettlitz edge and Upper Koettlitz Glacier sites, and Xanthomonadales at the Diamond Glacier (pH < 6) and Lower Koettlitz Glacier centre (Fig. S2, Supporting Information).

For Cyanobacteria, a total of 73 OTUs were delineated across all samples; the lowest number of sequences was obtained from the Diamond Glacier (pH < 6) site and the highest from the Diamond Glacier (pH > 6; Table 5). Samples from the Lower Koettlitz (edge) contained the most cyanobacterial OTUs and the highest species richness, Shannon–Wiener Index and Pielou Index (Table 5). The family Chamaesiphonaceae dominated in the Diamond (pH < 6; 73%) and Upper Koettlitz (66%) samples, and was the second most frequent in the Diamond pH > 6 (Fig. S2, Supporting Information). *Phormidium* sp. was the most abundant species in the other Upper Diamond Glacier CCHs (62%), *Leptolyngbya antarctica* dominated in the Lower Koettlitz centre CCHs (56%) and *Nostoc* sp. in Lower Koettlitz edge CCHs (32%; Fig. S2, Supporting Information).

Clone Libraries

Although the cyanobacterial clone libraries were only applied to a selection of the sample sets and captured less diversity than the HTS, a similar pattern in dominant cyanobacterial 16S rRNA gene diversity was observed with two *Chamaesiphon* taxa abundant in most samples, and *Phormidium*, or closely related taxa, abundant in one of the Diamond Glacier CCHs (Fig. S3, Table S3, Supporting Information).

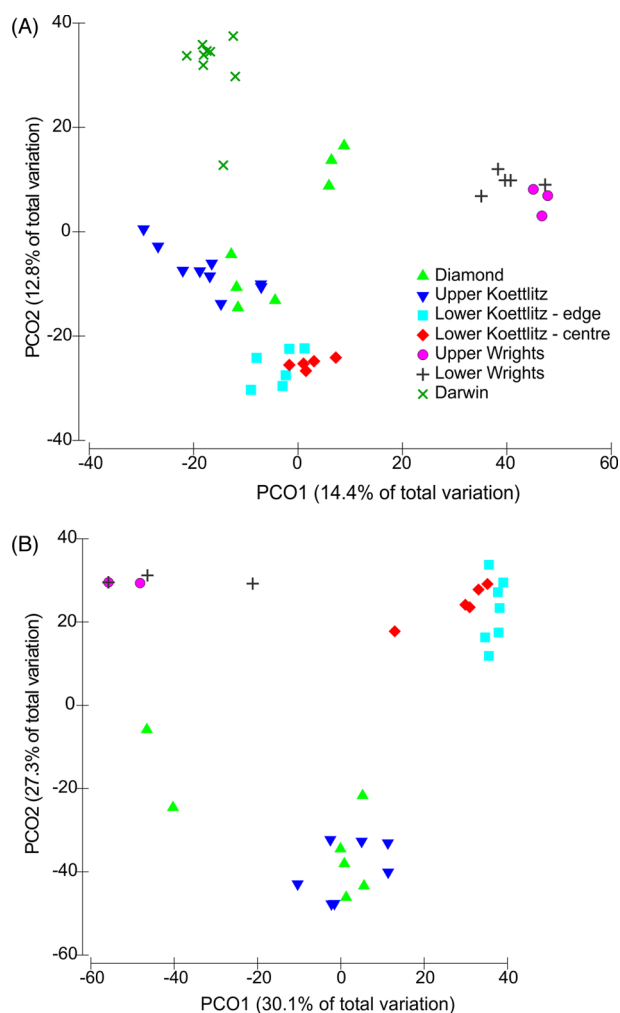


Figure 5. Principal Coordinated Ordination (PCO) based on Bray–Curtis similarities of ARISA of; (A) bacterial and, (B) cyanobacterial sediment communities in CCHs at the denoted glacier sites. Cyanobacteria-specific primers were not used on the Darwin Glacier samples.

Phylogenetic analysis of partial 16S rRNA genes generated in the clone libraries suggested that the cyanobacteria clustered with environmental sequences and isolates previously detected from Arctic and Antarctic freshwater and terrestrial soil environments including the McMurdo Dry Valleys. These analyses confirmed that sequences belonged to the genera *Chamaeosiphon*, *Pseudanabaena*, *Phormidesmis*, *Phormidium*, *Hormoscilla* and *Oscillatoria* (Fig. S4, Supporting Information).

DISCUSSION

CCHs are small aquatic ecosystems enclosed in glacier surface ice and are collectively an important part of the aquatic habitat of the inland Antarctic cryosphere. In this study, we investigated three hypotheses relating to the effects of entombment on CCH morphology and water chemistry, and how these factors may control sedimentary bacterial assemblages;

- (i) *There is greater variability in CCH physical environments between glacier sites and latitudes, than within a site, due to local differences in external environmental conditions.*

We might expect colder temperatures at higher altitudes to promote a thicker ice cover, thereby enhancing the isolation and longevity of the CCH water environment. For the CCH size range targeted in this study, a significantly thinner ice cover was evident at the Lower Wright and Lower Koettlitz Glacier sites, than at the respective upper glacier sites. Using the Cl flux model of Fountain et al. (2004) to estimate the length of time water in the CCH has been isolated, yielded mean isolation times of 10 years for Upper Wright Glacier CCHs, but only 5 years for Lower Wright Glacier CCHs. For the Koettlitz Glacier, where the altitude difference between the upper and lower glacier sites is even more pronounced, the very thin ice lid and likely partially open nature of the CCHs at the lower site, unfortunately precluded this type of estimation of isolation time.

The effects of latitude on CCH depth and ice thickness were less evident, possibly due to deliberate targeting of a specific cryoconite size range for this study. Certainly greater variability in ice thickness and depth was reported for glaciers in the Taylor Valley (e.g. Fountain et al. 2004), and Hodson et al. (2013) described CCH depths of up to 1 m from the margin of Eastern Antarctic Sheet. Open cryoconite holes described from the Arctic, Greenland and other alpine regions are often shallower (e.g. Hodson et al. 2008).

The nature of the sediment trapped in the CCH also appeared to reflect the regional environment. The lithology of sediment extracted from the Upper Koettlitz Glacier CCHs was similar to that of the ice-free landscape of the Upper Koettlitz Glacier area (Bull et al. 1961), and particle morphology was consistent with aeolian derivation.

- (ii) *There is greater variability in CCHs chemical characteristics within the different glacier sites, than between sites, due to factors linked to individual CCH genesis and evolution.*

The hypothesis assumes a common origin for the liquid water of all CCHs, in which water chemistry then evolves in response to internal CCH processes. The stable isotope signatures and low tritium concentrations, reminiscent of those in the glacial ice, indicate that the water in the CCHs is glacial ice melt, as previously proposed for Darwin Glacier cryoconites (Webster-Brown et al. 2010), and not derived from surface snow. The Lower Darwin Glacier site CCHs had a chemistry most reminiscent of unmodified glacial ice melt, with consistently low conductivity, low concentrations of all major ions and nutrients, and relatively light stable ^{18}O and D isotopic signatures. Nitrate concentrations, although higher than those at some of the other sites in this study, were within the concentration range exhibited by glacial ice at this site (Webster-Brown et al. 2010). Notably, Darwin Glacier ice nitrate concentration is higher than those reported for many Arctic glaciers in Svalbard and the Greenland Ice Sheet (Telling et al. 2011, 2012).

As CCHs age, major ion concentrations are anticipated to increase as the original glacial ice melt chemistry is affected by freeze concentration (ion exclusion as lid ice freezes), and weathering of entrained sediments. Highly variable CCH conductivity and major ion concentrations, within and between glacier sites, and covariance of major ions (except bicarbonate) with conductivity and chloride (e.g. Fig. 3) provide evidence of freeze concentration processes occurring. The extent of freeze concentration varies for each site, depending on the age of the cryoconite field. It is least pronounced for Lower Darwin CCHs, and apparently most pronounced for the Lower Koettlitz CCHs. However, in the Lower Koettlitz CCHs, periodic opening may enable higher ion concentrations to occur through evaporation and direct deposition of aerosol salts into the hole while open, as

Table 4. Results of multivariate multiple regression (DistLM) using bacterial ARISA data and environmental variables for; (A) each variable taken individually (ignoring other variables) and, (B) stepwise selection of variables, where amount explained by each variable added to model is conditional on variables already in the model (i.e. those variables listed above it). Prop: proportion of variance in species data explained by that variable; Cumul: cumulative proportion of variance explained.

(A) Marginal test	F	P	Prop.	
Dissolved Oxygen	4.44	0.001	0.096	
pH	5.29	0.001	0.112	
Sqr(HCO ₃)	2.82	0.001	0.063	
Log (Na+0.1)	5.55	0.001	0.117	
Log (Ca+0.1)	4.63	0.001	0.099	
Log (DRP+0.1)	3.30	0.001	0.073	
Log (NH ₄ +0.1)	3.38	0.001	0.075	
Log (NO ₃ +0.1)	4.21	0.001	0.091	
Log (DON+0.1)	1.32	0.122	0.030	
Log (DOP+0.1)	4.67	0.001	0.100	
Distance to sea	4.32	0.001	0.093	
Altitude	4.6747	0.001	0.100	
(B) Sequential tests	F	P	Prop.	Cumul.
Log (Na+0.1)	5.55	0.001	0.117	0.117
pH	5.95	0.001	0.112	0.229
Altitude	6.12	0.001	0.102	0.331
Dissolved Oxygen	3.59	0.001	0.056	0.387
Distance to sea	2.60	0.001	0.039	0.427
Log (DOP+0.1)	2.79	0.001	0.040	0.467

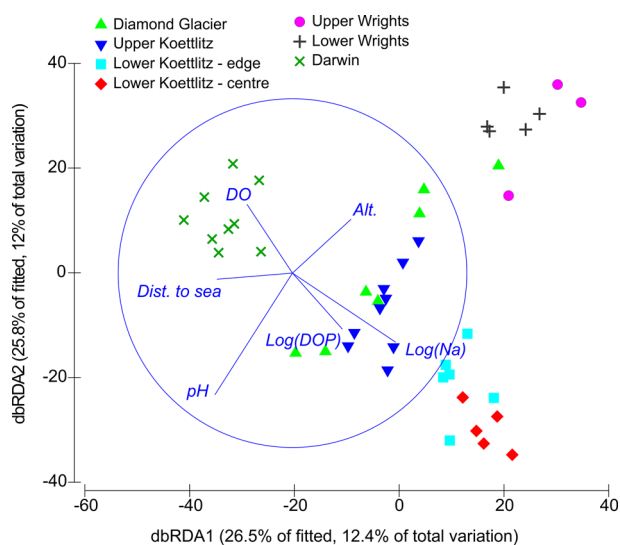


Figure 6. Redundancy analysis ordination plot on the basis of Bray–Curtis similarities of the ARISA bacterial data from sediment communities in CCHs at the denoted glacier sites. Vectors showing the best environmental predictors are overlaid. Alt. = altitude, DOP = dissolve organic phosphorus.

has been noted for open holes on the Canada Glacier in the Taylor Valley (Telling et al. 2014). The chemistry of Lower Koettlitz Glacier CCHs certainly appears to be more influenced by seawater than other sites, with higher Na and Cl, lower NO₃-N and a stable isotope signature very similar to that of seawater. It is also possible that the chemistry of these CCHs may be influenced by the presence of seawater lenses in the glacier, perhaps incorporated into the glacier where it extends out over the Ross Sea and merges with the McMurdo Ice sheet. Depleted NO₃-N has been consistently reported in other meltwater features close to open seawater, such as in ponds of the McMurdo Ice Shelf at Bratina

Island (Hawes et al. 1999), and of the Greenland Ice Sheet (Telling et al. 2012).

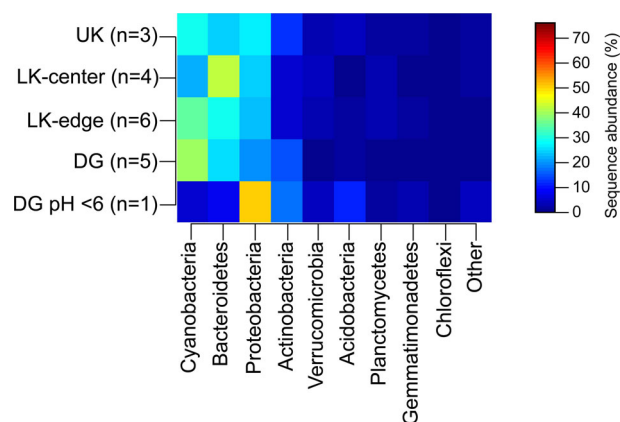
In situ biological processes, particularly photosynthesis, can exert an influence on pH and bicarbonate concentrations. Photosynthesis can raise pH to extreme levels in poorly buffered Antarctic meltwaters (e.g. Tranter et al. 2004; Hawes, Howard-Williams and Fountain 2008; Webster, Brown and Vincent 1994), and a wide range of pH was observed at all sites except the Lower Wright Glacier. A pH range of over almost six units was observed in Diamond Glacier CCHs, where holes with the lowest pH also had a very low number of cyanobacterial sequences, indicative of low levels of photosynthesis. Low pHs were also observed in the Lower (and some Upper) Wright Glacier CCH waters, where pH range was limited and therefore less influenced by photosynthesis. Bicarbonate concentrations can decrease in response to photosynthesis or low pH (loss as CO_{2(g)}), and increase through weathering of carbonate-bearing sediments, so concentrations are therefore more difficult to relate back to specific processes operating in the CCH.

- (ii) *Bacterial assemblages within CCHs are primarily derived from a common airborne pool of propagules in the Southern Victoria Land region, rather than from local sources, such that bacterial assemblages are similar for glaciers where similar growth conditions occur.*

The bacterial assemblages that we characterized generally grouped according to geographic location. A similar trend was observed by Cameron, Hodson and Osborn (2012) when comparing Arctic and Antarctic cryoconite microbial communities. Our data indicate that the diversity of CCH bacterial biota is unlikely to be derived from a common broadly spread inoculum, but is likely influenced by founder populations from more local sources in the McMurdo Dry Valleys and Southern Victoria Land. The exception is the overlap between the Upper Koettlitz and the Diamond Glacier CCHs, which are in different glacial catchments more than 200 km apart. However, both of these sites are

Table 5. Summary of mean biological parameters for bacterial and cyanobacterial (only) OTUs from cryoconite sediments at different geographic locations. Data presented are means.

Group	Location	n	No. of reads	No. of OTUs	Shannon diversity (H')	Richness (S)	Evenness (J)
Bacteria	Diamond pH > 6	5	33898	268	2.76	25.66	0.51
	Diamond pH < 6	1	33898	561	4.45	54.0	0.70
	Lower Koettlitz edge	6	33898	651	4.61	62.6	0.71
	Lower Koettlitz centre	4	33898	368	3.90	35.3	0.66
	Upper Koettlitz	3	33898	575	4.38	55.3	0.69
Cyano-bacteria	Diamond pH > 6	5	12870	11	0.62	1.1	0.24
	Diamond pH < 6	1	1319	12	1.08	1.5	0.44
	Lower Koettlitz edge	6	10655	45	2.36	4.7	0.62
	Lower Koettlitz centre	4	6735	21	1.08	2.3	0.36
	Upper Koettlitz	3	6914	24	1.29	2.6	0.41

**Figure 7.** Comparison of the relative composition of dominant bacterial phyla for cryoconite sediments at different geographic locations. Data presented are means, with n shown in parentheses. Phyla that accounted for less than 1% of the sequences across all samples were combined into 'others'. DG = Diamond Glacier, LK = Lower Koettlitz, UK = Upper Koettlitz.

at relatively high altitude, with broadly open drainage from the polar plateau from which radial winds typically blow (Parish and Bromwich 1987, 2007). The prevalence of such drainage winds means that these sites may be effectively receiving the same air mass, and their similarity may therefore reflect this common propagule source. In this case, the propagule source is likely to be more widely distributed, rather than dominated by in-valley sources.

By contrast, the Upper Wright Glacier is enclosed in a deeply incised valley, within which up- and down-valley winds are common, so common in-valley propagule sources are likely (Doran et al. 2002). The observation of close linkage of the two Wright Valley sites, and separation from other valleys and the high-altitude sites, is therefore consistent with valley-localized dispersal of biota. This is consistent with Lee et al. (2012), who observed that bacterial diversity in different McMurdo Valleys was highly localized, and most likely driven by physicochemical factors specific to those locations. Such patchy terrestrial bacterial diversity may influence cryoconite bacterial assemblages downwind. Similarities between bacterial communities in supraglacial meltwaters in the Lower Darwin Glacier and adjacent ice-free terrestrial ponds, have previously been reported for the Darwin Valley (Webster-Brown et al. 2010) and attributed to such cross-fertilisation. Mindl et al. (2007) and Stibal et al. (2015) suggested a similar local seeding of glacier habitats in high Arc-

tic Svalbard and the Greenland Ice sheet respectively, though other work by Edwards et al. (2011, 2013a,b) described distinctive differences in bacterial and fungal assemblages between cryoconite and glacier margin habitats in the Arctic (Edwards et al. 2013a,b)

Cyanobacteria are often the most abundant primary producers in Antarctic freshwater ecosystems (Vincent 2000, Zakhia et al. 2009); a feature also noted in some of the CCHs in this study. Cyanobacteria have previously been reported to be abundant in Arctic and Antarctica cryoconite holes based on molecular studies (Christner et al. 2005; Takeuchi, Nishiyama and Zhongqin 2010; Cameron, Hodson and Osborn 2012; Edwards et al. 2014; Stibal et al. 2015). HTS-based community richness was lower than that of cyanobacterial communities described from another HTS-based study at Antarctic Peninsula (Kleinteich et al. 2014). A geographic pattern was observed across the Wright, Diamond and Koettlitz Glacier sites, with distinct cyanobacterial compositions noted at each site. One difference in the cyanobacterial assemblages in CCHs of the Diamond (pH < 6) and Upper Koettlitz Glacier sites, compared to those of other CCHs in our dataset and those previously described in terrestrial pond ecosystems from this region, was the low frequency of Oscillatoriales and dominance by the unicellular Chamaesiphonaceae. Terrestrial meltwater ponds and lakes in Antarctica are usually dominated by the thin Oscillatorian filamentous genus *Leptolyngbya*, and unicellular forms tend to be rare (Jungblut et al. 2005; Jungblut, Vincent and Lovejoy 2012). Previous analysis 16S rRNA gene of open cryoconite hole sediments failed to detect *Leptolyngbya* in Arctic and Antarctic cryoconites, but showed the presence of sequences belonging to *Chaemosiphon*, *Phormidium* and *Nostoc* (Christner, Kvitoko and Reeve 2003; Edwards et al. 2014), although both studies screened only a small number of cyanobacterial sequences. *Leptolyngbya* was, however, present in variable abundance in our samples and was dominant in the Lower Koettlitz centre CCHs. Nostocales OTU abundance was variable, and significant only at the Lower Koettlitz Glacier edge site (ca. 30%, and comprised mostly of *Nostoc* sp.), confirming the ability of both *Leptolyngbya* and *Nostoc* to colonize and grow in such habitats. The Lower Koettlitz edge site had the highest cyanobacterial richness (as measured with HTS) and local influences may include the terrestrial meltwater ponds of the nearby Miers Valley and McMurdo Ice Shelf which are rich in Nostocales (Jungblut et al. 2005). More frequent melting of the lid ice at these lower elevation cryoconites, would facilitate wind transfer of cyanobacteria from terrestrial pond environments.

Growth periods in CCH holes may be short, but our data suggest that closed holes may have sufficient longevity and

isolation for a consistent, niche-like relationship to an environmental variable (such as pH) to override any founder effects of the initial inoculum. The largest within-site range of growth conditions was seen on the Diamond Glacier, where pH ranged over six units. In this case distinct bacterial assemblages were evident in CCHs of pH < 6, and those with neutral-alkaline pH. The bacteria community from pH < 6 CCHs, showed a very low proportion of cyanobacteria and higher proportions of Proteobacteria and Acidobacteria. The PCO analysis grouped the low pH CCHs from the two Wright Valley glaciers with those from the Diamond, supporting the view that selection by pH was driving community composition in a consistent, cross-valley way. The presence of such low pH cryoconites, with a distinctive bacterial community, has not previously been reported for open cryoconite holes in the Arctic or Antarctic. Open cryoconites will have a greater pH buffering capacity, due to contact with air, snow and possible hydrodynamic connection with other meltwaters, as well as ongoing access to airborne propagules from local sources.

The multivariate multiple regression analysis combining biological and physicochemical data, further supports the hypothesis that the growth environment affects bacterial community structure. The sequential stepwise selection of variables identified a combination of six physicochemical factors that explained greater than 46% of the observed differences in bacterial assemblages. Half of the predictive power was vested in pH and Na, with the latter representing broader major ion chemistry through the observed ion covariance. While cross-site confirmation of the structuring effect of pH is apparent, evaluation of other variables must take account of the tendency for sites to have inherently different properties, which may confound environmental and founder population effects. The effect of Na for example, is largely driven by an axis between the potentially marine-affected Lower Koettlitz and the highly dilute Darwin glaciers. However, the ability to explain a substantial proportion of bacterial community variation, both within and between sites, based on environmental variables does support the view that, in addition to founder effects, bacterial communities are also structured by their growth environment.

CONCLUSIONS

Our first hypothesis, that the physical environments in the CCHs is controlled largely by differences in external environmental conditions between the sites, was supported in so far that all sites showed similar CCH depths, which we infer to reflect similar insolation, while ice lid thickness varied with altitude. The latter was, however, most evident at the Lower Koettlitz Glacier sites, which were also chemically distinct and relatively close to the coast, and this may have confounded altitude effects. The second hypothesis, that chemical characteristics varied significantly between CCHs at each glacier site, due to differences in individual CCH genesis, was supported. Key determinants in the chemical evolution of the individual CCH were glacial ice chemistry, the time of isolation (or frequency of opening events) and therefore extent of freeze concentration effects, and the extent of biological (principally photosynthetic) processes.

However, the third hypothesis, that bacterial assemblages within CCHs are primarily derived from a common airborne pool of propagules rather than from local sources and differences, was not supported. CCH bacterial assemblages appear to be significantly influenced by a local, presumably airborne, pool of propagules with clear geographic trends and organisms

in common with local terrestrial freshwater aquatic systems. A relationship between growth environment (in particular the pH and major ion concentrations) was also identified as explaining inter-valley variability to a significant degree.

Our results imply that CCHs preserve a fingerprint of the local or regional bacterial assemblages, modified by their evolution in an isolated environment in which the chemistry can vary significantly. This patchwork ecosystem, distributed across glacier surfaces, contributes to the freshwater bacterial taxonomic and potentially metabolic, diversity of the glacier catchment. They should be considered as quantitatively and qualitatively significant components of a fragmented but linked aquatic component of icy polar landscapes.

SUPPLEMENTARY DATA

Supplementary data are available at FEMSEC online.

ACKNOWLEDGEMENTS

The logistics support and facilities in Antarctica were provided by Antarctica New Zealand. We thank Stephen Russell (Natural History Museum) for his help with the molecular work, and two anonymous reviewers for insightful comments and suggestions, Travis Horton (University of Canterbury) for stable isotope analysis, Louis Ranjard (New Zealand Genomics Limited) for bioinformatics assistance, Javier Atalah (Cawthron) for statistical advice, and Lisa Peacock (Cawthron) for help with Fig. 1.

Conflict of interest. None declared.

REFERENCES

- Abdo Z, Schütte UME, Bent SJ, et al. Statistical methods for characterizing diversity of microbial communities by analysis of terminal restriction fragment length polymorphisms of 16S rRNA genes. *Environ Microbiol* 2006;**8**:929–38.
- Abyzov SS. Microorganisms in Antarctic ice. In: Friedman EI (ed.). *Antarctic Microbiology*. New York: Wiley, 1993, 265–96.
- Altschul SF, Gish W, Miller W, et al. Basic local alignment search tool. *J Mol Biol* 1990;**215**:403–10.
- Anderson MJ. A new method for non-parametric multivariate analysis of variance. *Aust Ecol* 2001;**26**:32–46.
- Anderson MJ, Gorley RN. PERMANOVA+ for primer: guide to statistical methods. Plymouth: PRIMER-E, 2007.
- Anesio AM, Hodson AJ, Fritz A, et al. High microbial activity on glaciers: importance to the global carbon cycle. *Glob Change Biol* 2009;**15**:955–60.
- Bagshaw EA, Tranter M, Fountain AG, et al. Biogeochemical evolution of cryoconite holes on Canada Glacier, Taylor Valley, Antarctica. *J Geophys Res* 2007;**112**:G04S35.
- Bull CBB, Wheeler RH, Willis IAG, et al. *Geology Report of the Victoria University of Wellington Antarctic Expedition 1960–1961*. VUWAE 4. Wellington: Victoria University of Wellington, 1961.
- Cameron KA, Hodson AJ, Osborn AM. Structure and diversity of bacteria, eukaryotic and archaeal communities in glacial cryoconite holes from the Arctic and the Antarctic. *FEMS Microbiol Ecol* 2012;**91**:254–67.
- Caporaso JG, Lauber CL, Walters WA, et al. Global patterns of 16S rRNA diversity at a depth of millions of sequences per sample. *P Natl Acad Sci USA* 2011;**108**:4516–22.
- Cardinale ML, Brusetti P, Quatrini S, et al. Comparison of different primer sets for use in automated ribosomal intergenic

- spacer analysis of complex bacterial communities. *Appl Environ Microb* 2004;**70**:6147–56.
- Castello JD, Rogers SO (eds). *Life in Ancient Ice*. Princeton, NJ, USA: Princeton University Press, 2005.
- Christner BC, Kvitoko BH, Reeve JN. Molecular identification of Bacteria and Eukarya inhabiting an Antarctic cryoconite hole. *Extremophiles* 2003;**7**:177–83.
- Christner BC, Mosely-Thomson E, Thomson LG, et al. Classification of bacteria from polar and non-polar glacial ice. In: Castello JD, Rogers SO (eds). *Life in Ancient Ice*. Princeton, NJ, USA: Princeton University Press, 2005, 227–39.
- Doran PT, McKay CP, Clow GD, et al. Valley floor climate observations from the McMurdo Dry Valleys, Antarctica, 1986–2000. *J Geophys Res* 2002;**107**:4772.
- Edgar RC, Haas BJ, Clemente JC, et al. UCHIME improves sensitivity and speed of chimera detection. *Bioinformatics* 2011;**27**:2194–200.
- Edwards A, Anesio AM, Rassner SM, et al. Possible interactions between bacterial diversity, microbial activity and supraglacial hydrology of cryoconite holes in Svalbard. *ISME J* 2011;**5**:150–60.
- Edwards A, Douglas B, Anesio AM, et al. A distinctive fungal community inhabiting cryoconite holes on glaciers in Svalbard. *Fungal Ecol* 2013a;**6**:168–76.
- Edwards A, Rassner SM, Anesio AM, et al. Contrasts between cryoconite and ice-marginal bacterial communities of Svalbard glaciers. *Polar Res* 2013b;**32**:1–9. <http://dx.doi.org/10.3402/polar.v32i0.19468>.
- Edwards A, Mur LAJ, Girdwood SE, et al. Coupled cryoconite ecosystem structure-function relationships are revealed by comparing bacterial communities in alpine and Arctic glaciers. *FEMS Microbiol Ecol* 2014;**89**:222–37.
- Foreman CM, Sattler B, Mikucki J, et al. Metabolic activity and diversity of cryoconites in the Taylor Valley, Antarctica. *J Geophys Res* 2007;**112**:1–11, DOI: 10.1029/2006JG000358.
- Fountain AG, Nylen TH, Tranter M, et al. Temporal variations in physical and chemical features of cryoconite holes on Canada Glacier, McMurdo Dry Valleys, Antarctica. *J Geophys Res* 2008;**113**:1–11, DOI: 10.1029/2007JG000430.
- Fountain AG, Tranter M, Nylen TH, et al. Evolution of cryoconite holes and their contribution to meltwater runoff from glaciers in the McMurdo Dry Valleys, Antarctica. *J Glaciol* 2004;**50**:35–45.
- Gribbon PW. Cryoconite holes on Sermikaysak, West Greenland. *J Glaciol* 1979;**22**:177–81.
- Hawes I, Howard-Williams C, Fountain AG. Ice-based freshwater ecosystems. In: Vincent WF, Laybourn-Parry J (eds). *Polar Lakes and Rivers*. Oxford: OUP, 2008, 103–18.
- Hawes I, Smith R, Howard-Williams C, et al. Environmental conditions during freezing and response of microbial mats in ponds of the McMurdo Ice Shelf, Antarctica. *Antarct Sci* 1999;**11**:198–208.
- Hodson AJ, Anesio AM, Tranter M, et al. Glacial ecosystems. *Ecol Monogr* 2008;**78**:41–67.
- Hodson A, Paterson H, Westwood K, et al. A blue-ice ecosystem on the margins of the East Antarctic ice sheet. *J Glaciol* 2013;**59**:255–68.
- Huber JA, Faulkner G, Hugenholtz P. Bellerophon; a program to detect chimeric sequences in multiple sequence alignments. *Bioinformatics* 2004;**20**:2317–9.
- Jungblut AD, Hawes I, Hitzfeld B, et al. Diversity within cyanobacterial mat communities in variable salinity meltwater ponds of McMurdo Ice Shelf, Antarctica. *Environ Microbiol* 2005;**7**:519–29.
- Jungblut A-D, Hawes I, Mountfort D, et al. Diversity within cyanobacterial mat communities in variable salinity meltwater ponds of McMurdo Ice Shelf, Antarctica. *Environ Microbiol* 2005;**7**:519–29.
- Jungblut AD, Lovejoy C, Vincent WF. Global distribution of cyanobacterial ecotypes in the cold biosphere, *ISME J* 2010;**4**:191–202.
- Jungblut AD, Vincent WF, Lovejoy C. Eukaryotes in Arctic and Antarctic cyanobacterial mats. *FEMS Microbiol Ecol* 2012;**82**:416–28.
- Kleinteich J, Hildebrand F, Wood SA, et al. Diversity of toxin and non-toxin containing cyanobacterial mats of meltwater ponds on the Antarctic Peninsula: a pyrosequencing approach. *Antarct Sci* 2014;**26**:521–32.
- Larkin MA, Blackshields G, Brown NP, et al. Clustal W and Clustal X version 2.0. *Bioinformatics* 2007;**23**:2947–8.
- Lee CK, Barbier BA, Bottos EM, et al. The inter-valley soil comparative survey: the ecology of Dry Valley edaphic microbial communities. *ISME J* 2012;**6**:1046–57.
- Legendre P, Anderson MJ. Distance-based redundancy analysis: testing multispecies responses in multifactorial ecological experiments. *Ecol Mono* 1999;**69**:1–24.
- McDonald D, Price MN, Goodrich J, et al. An improved Greengenes taxonomy with explicit ranks for ecological and evolutionary analyses of bacteria and archaea. *ISME J* 2012;**6**:610–8.
- Maddison DR, Maddison WP. *MacClade: analysis of phylogeny and character evolution*, v. 4.08. 2005. Sunderland MA: Sinauer Associates.
- Mindl B, Anesio AM, Meirer K, et al. Factors influencing bacterial dynamics along a transect from supraglacial runoff to proglacial lakes of a High Arctic glacier. *FEMS Microbiol Ecol* 2007;**59**:307–17.
- Mueller D, Vincent WF, Pollard WH, et al. Glacial cryoconite ecosystems: A bipolar comparison of algal communities and habitats. *Nova Hedwigia* 2001;**123**:173–97.
- Nkem JN, Wall DH, Virginia RA, et al. Wind dispersal of soil invertebrates in the McMurdo Dry Valleys, Antarctica. *Polar Biol* 2006;**29**:346–52.
- Parish TR, Bromwich DH. The surface windfield over the Antarctic ice sheets. *Nature*, 1987;**328**:51–4.
- Parish TR, Bromwich DH. Reexamination of the near-surface airflow over the Antarctic continent and implications on atmospheric circulations at high southern latitudes. *Mon Weather Rev* 2007;**135**:1961–73.
- Porazinska DL, Fountain AG, Nylen TH, et al. The biodiversity and biogeochemistry of cryoconite holes from McMurdo Dry Valley Glaciers, Antarctica. *Arc, Ant Alp Res* 2004;**36**:84–91.
- Pruesse E, Quast C, Knittel K, et al. SILVA: a comprehensive online resource for quality checked and aligned ribosomal RNA sequence data compatible with ARB. *Nucleic Acids Res* 2007;**35**:7188–96.
- Schloss PD, Westcott SL, Ryabin T, et al. Introducing Mothur: open-source, platform-independent, community-supported software for describing and comparing microbial communities. *Appl Environ Microb* 2009;**75**:7537–41.
- Stamatakis A, Hoover P, Rougemont J. A Rapid Bootstrap Algorithm for the RAxML Web Servers. *Syst Biol* 2008;**57**:758–71.
- Stibal M, Schostag M, Cameron KA, et al. Different bulk and active bacterial communities in cryoconite from the margin and interior of the Greenland ice sheet. *Environ Microbiol Rep* 2015;**7**:293–300.

- Takeuchi N, Nishiyama H, Zhongqin L. Structure and formation process of cryoconite granules on Urumqi glaciers No. 1, Tien Shan, China. *Ann Glaciol* 2010;51:9–14.
- Tranter M, Fountain AG, Fritsen CH, et al. Extreme hydrochemical conditions in natural microcosms entombed within Antarctica ice. *Hydrol Process* 2004;18:379–87.
- Telling J, Anesio AM, Tranter M, et al. Nitrogen fixation on Arctic glaciers, Svalbard. *J Geophys Res* 2011;116:G03039.
- Telling J, Anesio AM, Tranter M, et al. Spring thaw ionic pulses boost nutrient availability and microbial growth in entombed Antarctic Dry Valley cryoconite holes. *Frontiers Microbiol* 2014;5:1–15, DOI: 10.3389/fmicb.2014.00694.
- Telling J, Stibal M, Anesio AM, et al. Microbial nitrogen cycling on the Greenland Ice Sheet. *Biogeosciences* 2012;9:2431–42.
- Vincent WF. Cyanobacterial dominance in polar regions. In: Whitton BD, Potts M (eds). *The Ecology of Cyanobacteria*. The Netherlands: Kluwer Academic Publishers, 2000, 321–40.
- Vincent WF, Howard-Williams C. Nitrate-rich waters of the Ross Ice Shelf region. *Antarct Sci* 1994;6:339–46.
- Waters JM, Fraser CI, Hewitt GM. Founder takes all: density-dependent processes structure biodiversity. *TREE* 2013;28:78–85.
- Webster-Brown J, Gall M, Gibson J, et al. The biogeochemistry of meltwater ponds in the Darwin Glacier region (Lat 80°S), Victoria Land. *Antarct Sci* 2010;22:646–61.
- Webster JG, Brown KL, Vincent WF. Chemistry and nutrient content of meltwaters of the Victoria Valley, Antarctica. *Hydrobiologia* 1994;281:171–86.
- Wharton RA, McKay CP, Simmons GM, et al. Cryoconite holes on glaciers. *Bioscience* 1985;35:499–503.
- Wood SA, Casas M, Taylor DI, et al. Changes in tetrodotoxin concentrations and bacterial communities in *Pleurobranchia maculata* and egg masses and when maintained in captivity. *J Chem Ecol* 2012b;38:1342–50.
- Wood SA, Kuhajek J, de Winton M, et al. Species composition and cyanotoxin production in periphyton mats from three lakes of varying trophic status. *FEMS Microbiol Ecol* 2012a;79:312–26.
- Wood SA, Rueckert A, Cowan D, et al. Sources of edaphic cyanobacterial diversity in the Dry Valleys of Eastern Antarctica. *ISME J* 2008;2:308–20.
- Zakhia F, Jungblut AD, Taton A, et al. Cyanobacteria in cold environments. In: Margesin R, Schinner F, Marx JC, Gerday C (eds). *Psychrophiles: From Biodiversity to Biotechnology*. Berlin: Springer-Verlag, 2009, 121–35.